JACS
JOURNAL OF THE AMERICAN CHEMICAL SOCIETY
pubs.acs.org/JACS
Communication

Synthesis and Interlayer Assembly of a Graphenic Bowl with Peripheral Selenium Annulation

Zhen-Lin Qiu,[#] Yang Cheng,[#] Qi Zeng, Qiong Wu, Xin-Jing Zhao, Rong-Jie Xie, LiuBin Feng, Kaihui Liu,[*] and Yuan-Zhi Tan[*]

Cite This: https://doi.org/10.1021/jacs.2c12401
Read Online
ACCESS | Metrics & More | Article Recommendations | Supporting Information

ABSTRACT: Pentagonal cyclization at the bay positions of armchair-edged graphenic cores can build molecular bowls without the destruction of hexagonal lattices. However, this synthesis remains challenging due to unfavorable strain and the multiple reactions required. Here, we show that a new type of graphenic molecular bowl with a depth of 1.7 Å and a diameter of 1.2 nm is constructed by sextuple Se annulation at the bay positions of armchair-edged hexa-peri-hexabenzocoronene. This graphenic bowl is functionalized with phenylseleno groups that stack into a discrete bilayer dimer in solution. Such a dimer exhibits high stability and survives in the gas phase after laser ablation. Strikingly, the asymmetric one-dimensional supramolecular columns of graphenic bowl with coherent stacking configuration are observed in the solid state, which results in a strong second harmonic generation with prominent polarization dependence. Our findings present a concise synthesis of a giant molecular bowl with a graphenic core and demonstrate the unique supramolecular assembly of extended graphenic bowls.

Bowl-shaped nanocarbons are a segment of curved carbon nanomaterials that include fullerenes, carbon nano-onions, and the cap of carbon nanotubes.[1−3] As a result of their asymmetrical π-conjugated systems, bowls exhibit intriguing properties such as chirality,[4−6] dynamic bowl inversion,[7−10] ferroelectricity,[11−13] and supramolecular recognition.[14−21] The key to achieving the bowl shape is the incorporation of pentagons into the carbon skeleton.[22,23] Structurally, the pentagons are located at the inner core of the carbon skeleton, as in the case of corannulene,[24−27] which is different from the honeycomb network of graphene.[28] Alternatively, the construction of pentagons at the periphery of the carbon backbone can result in a bowl-shaped structure without the destruction of graphenic networks.[29,30] For example, the bowl-shaped molecule, sumanene,[31,32] is composed of a triphenylene core and three pentagons at the periphery of the triphenylene (Figure 1). Triphenylene can be regarded as the smallest cutout of graphenic networks with full armchair edges. The pentagonal cyclization of the bay positions in other armchair graphenic aromatic hydrocarbons[33] such as hexa-peri-hexabenzocoronene (HBC) results in extended graphenic molecular bowls. This strategy is an alternative pathway to a class of molecular bowls composed of a graphenic core and pentagonal peripheries. However, the introduction of multiple pentagons into a planar graphenic core is synthetically challenging because of unfavorable strain and multiple pentagonal cyclizations.[23] In this manuscript, we use this strategy to synthesize a graphenic molecular bowl, hexa-selenium annulated hexa-peri-hexabenzocoronene (HSHBC).

The synthesis of HSHBC was feasibly achieved through the nucleophilic substitution of perchlorinated HBC (PCHBC) with diphenyl diselenide. The structure of HSHBC was unequivocally identified using single crystal X-ray diffraction (SCXRD). The SCXRD analysis reveals a bowl-shaped structure with a depth of 1.7 Å and a diameter of 12 Å. Remarkably, HSHBC with phenylseleno groups (**1**) assembles into a discrete bilayer structure in solution as evidenced by nuclear magnetic resonance (NMR) spectroscopies. Mass spectroscopic measurements reveal that the bilayer dimer of **1** is stable in the gas phase as well. In the solid state, **1** stacks into synclastic one-dimensional columns and forms polarized

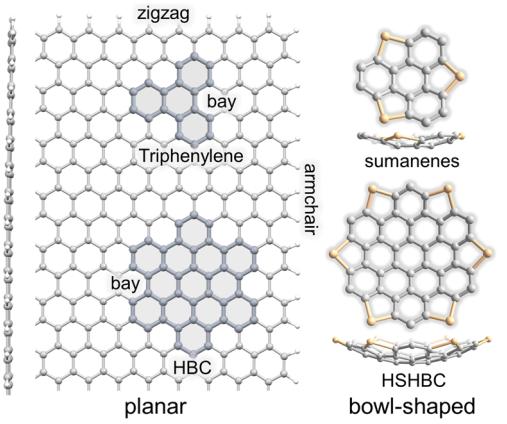

Figure 1. Pentagonal cyclization at the bay positions of armchair-edged graphenic cutouts.

Received: November 22, 2022

crystals in the *P6cc* space group. The crystals of **1** exhibit a strong second harmonic generation (SHG) response with prominent polarization dependence.

Cyclizing the bay position with chalcogen atoms is a promising way to introduce the pentagonal ring at the periphery of aromatic hydrocarbons, as demonstrated by the synthesis of trichalcogenasumanenes.[34−37] The previous work showed that the nucleophilic thiolation of PCHBC formed three thiophene rings at the bay positions of the HBC core, producing trisulfur-annulated HBC.[38] The trisulfur-annulated HBC still possesses a quasi-planar structure, and products with further S annulation were not observed, probably due to the high strain involved. Inspired by the easier formation of triselenasumanene than trithiasumanene,[34,35] the nucleophilic thiolation of PCHBC was replaced by selenolation in an attempt to achieve full annulation at the bay positions of HBC core. Following this step, PCHBC was reacted with diphenyl diselenide using DMI as the solvent in the presence of NaOH (Figure 2a). After reaction, the product was isolated and

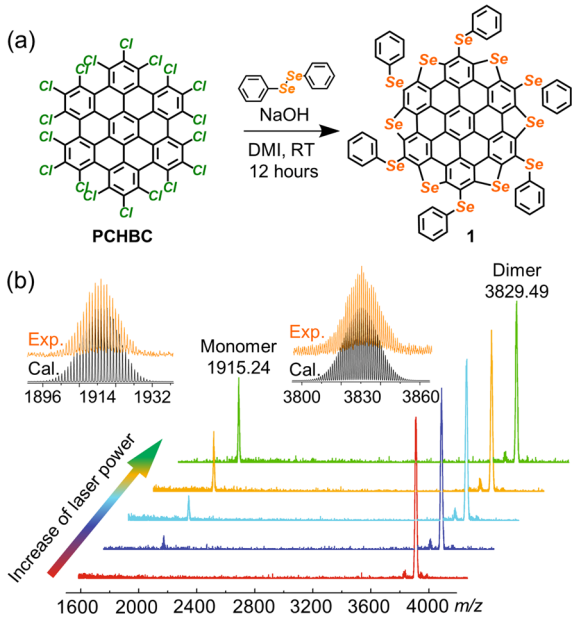

Figure 2. Synthetic route and mass spectra of **1**. (a) Synthetic route for **1**. (b) Mass spectra of **1** with different desorption laser powers. The isotopic distributions of the mass peak are shown as the insets.

purified using the silica column and high-performance liquid chromatography (HPLC) (see the Supporting Information S1−S2). As expected, sextuple annulation of Se occurred at the bay positions of HBC, while six phenylseleno groups were substituted at the vertexes, yielding hexakis(phenylseleno) HSHBC (**1**) (Figure 2a).

The purified product was analyzed by matrix-assisted laser desorption/ionization-time-of-flight (MALDI-TOF) mass spectrometry (Figure 2b). The MALDI-TOF mass spectrum possesses a single peak with a mass/charge ratio value of 3829.49 Da. The found mass and isotopic pattern exactly match the molecular formula of the dimer of **1** $(C_{78}H_{30}Se_{12})_2$. This result indicates that **1** forms dimers by supramolecular assembly, and this dimer is stable enough to survive laser ablation. As the laser power increases, an additional peak appears at 1915.24 Da, which is assigned to the monomer **1**. The peak intensity of the monomer increases with greater laser power, indicating that the dimer $(\mathbf{1})_2$ dissociates into corresponding monomers as a result of laser ablation, which is consistent with the supramolecular binding of $(\mathbf{1})_2$.

The structure of **1** was further investigated by ^{1}H NMR spectroscopy. Its ^{1}H NMR spectrum consists of five peaks with an intensity ratio of 2:3:2:1:2 (Figure 3a, Figure S1), clearly

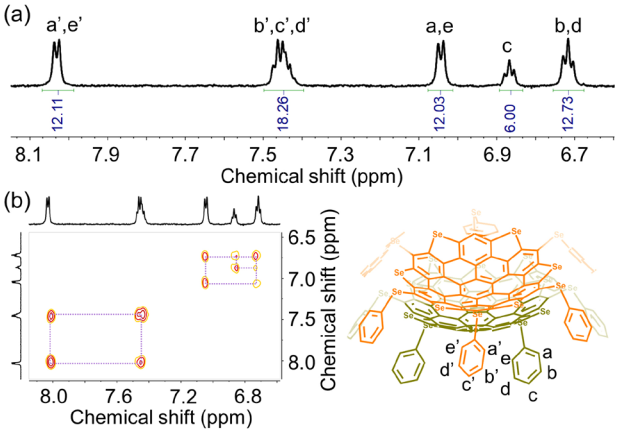

Figure 3. NMR characterization of **1**. (a) ^{1}H NMR spectrum of $(\mathbf{1})_2$ measured in $C_2D_2Cl_4$. Signal assignment is aided by 2D NMR spectroscopy. (b) ^{1}H−^{1}H COSY NMR spectrum of $(\mathbf{1})_2$ measured in $C_2D_2Cl_4$.

different from the monomeric structure of **1**. We speculate that $(\mathbf{1})_2$ is the dominant species in solution, as observed in the gas phase in mass spectra (Figure 2b). In the ^{1}H−^{1}H correlated spectroscopy (COSY) NMR spectrum (Figure 3b), the five peaks are grouped into two sets of signals, corresponding to two kinds of phenyl rings that belong to the two different layers in $(\mathbf{1})_2$, which agrees with the ^{13}C and ^{13}C−^{1}H COSY spectra (Figures S2−S3). The 2D nuclear Overhauser effect spectroscopy (NOESY) NMR spectra (Figure S4) demonstrated the short interactions between phenyl rings from different layers, confirming the stacked structure. The bilayer architecture of $(\mathbf{1})_2$ was further corroborated by diffusion-ordered 2D-NMR spectroscopy (DOSY) (Figure S5). The ^{1}H signals were at the same diffusion band with a diffusion coefficient (D) at 2.17×10^{-10} m^2/s, which is close to that of the reported bilayer nanographene[39] $(C_{96})_2$ (Mw = 3784.3, D = 2.37×10^{-10} m^2/s) (Figure S5b), suggesting their comparable molecular weight. Variable-temperature and variable-concentration ^{1}H NMR spectra did not show obvious changes, indicating that the bilayer structure of $(\mathbf{1})_2$ is highly stable (Figures S6−S7).

$(\mathbf{1})_2$ shows three absorption bands that peak at 440, 481, and 550 nm, red-shifted by 90 nm, compared with pristine HBC. The absorption bands can be assigned to the β, p, and α bands, respectively. The extinction coefficient of $(\mathbf{1})_2$ was measured to be 1.83×10^5 M^{-1} cm^{-1} at 440 nm. The optical energy gap (E_{opt}), derived from the p-band,[40] was 2.58 eV for $(\mathbf{1})_2$, smaller than that of HBC (3.18 eV). The decreased energy gap of $(\mathbf{1})_2$ originates from the extended conjugation due to multiple Se annulation. $(\mathbf{1})_2$ emitted an orange fluorescence at 563 nm (Figure S8), but the quantum yield is quite low (0.2%), owing to the heavy atom effect of Se. Concentration-dependent absorption and emission spectra exhibit negligible alteration as well (Figure S9), validating the stability of dimeric $(\mathbf{1})_2$ in the solution. $(\mathbf{1})_2$ has two reduction waves at −1.65 and −2.37 V vs Fc$^+$/Fc and three oxidation

https://doi.org/10.1021/jacs.2c12401
J. Am. Chem. Soc. XXXX, XXX, XXX−XXX

waves at 0.95, 1.29, and 1.61 V vs Fc^+/Fc (Figure S11 and Table S1). The first reduction for $(\mathbf{1})_2$ is about 0.47, 0.45, and 0.31 V more positive than that of hexa-dodecyl-HBC,[41] hexa-*tert*-butyl-HBC,[42] and dodeca-fluorine substituted HBC,[43] respectively. The better electronic accepting of $(\mathbf{1})_2$ is probably due to stabilization of the negative charges by the annulated Se atoms and peripheral phenylseleno groups. The electrochemical energy gap of $(\mathbf{1})_2$ was estimated to be 2.60 eV, in consistence with its E_{opt}.

The structure of **1** revealed by SCXRD (Figure 4 and Supporting Information S3) shows the distinguishable bowl-shaped structure with sextuple Se annulation at the bay positions. The incorporation of pentagons at the bay positions of armchair graphenic molecules convert the planar skeleton into bowls. The depth of the bowl of **1** is 1.74 Å, much deeper than that of corannulene[25] (0.87 Å) and sumanene[32] (1.11 Å) due to the enlarged molecular size. Theoretical calculations indicate that the bowl-inversion barrier of **1** is about 22 kcal/mol, larger than that of sumanene[44] and corannulene,[7] as result of its increased depth. Notably, **1** forms one-dimensional columns along the *c*-axis in the crystalline state rather than the dimeric stacking observed in the solution or gas phase (Figure 4c, Figure S12). In the stacking structure of **1**, a series of Se···π (3.59 Å) and Se···Se (3.64 Å) short contacts were observed (Figure S13). The intermolecular interactions in $(\mathbf{1})_2$ visualized by the independent gradient model based on the Hirshfeld partition (IGMH) method (Figures S14–S15) reveal the attractive Se···π and Se···Se interactions. The theoretical calculations of interaction energies also confirmed the strong interactions between phenylseleno groups (Supporting Information S4). The Se-involved intermolecular interactions, associated with interlayer $\pi-\pi$ interactions, could account for the interlayer stacking of **1** both in the solution and in the solid state.[45,46]

The stacked columns of **1** align in the same direction, leading to a noncentrosymmetric space group *P6cc* for the crystals of **1**. Therefore, their SHG properties were investigated (Figure 5a). The crystals of **1** have an elongated hexagonal prism shape, and the long axis of elongated hexagonal prism crystal aligns with the packing direction of the supramolecular column (Figure 5b) determined by SCXRD. Thermogravimetric analysis (TGA) (Figure S16) showed the thermal stability of **1** up to 360 °C under inert atmosphere. These crystals were fabricated by spin coating onto a fused silica substrate (Figure 5b). Under excitation at frequency ω, the second-order susceptibility $\chi^{2\omega}$ brings about nonlinear polarization $p^{2\omega} = \varepsilon_0\chi^{2\omega}E^{\omega}E^{\omega}$, where ε_0 is the permittivity of free space and E^{ω} is the incident electric field. With a 1380 nm femtosecond pulse-laser excitation, the crystals of **1** exhibit a sharp peak at 690 nm as expected for SHG (Figure 5c).

To quantify the SHG of the crystals of **1**, the SHG intensities of a WS_2 monolayer and a hBN monolayer were measured for comparison. Usually, the 2D monolayer materials possess stronger SHG intensity than materials in the bulk or those consisting of a few layers.[47,48] The crystals of **1** and WS_2 monolayer were measured using a pump fluence of 37.8 mJ/cm^2, while a fluence of 84 mJ/cm^2 was used for the hBN monolayer because its SHG response is weak compared to that of **1**. Strikingly, a strong SHG for the crystal of **1** was observed, which is a few times higher than that for the WS_2 monolayer. The damage threshold power for the crystal of **1** using the 1380 nm laser is similar to that of the WS_2 monolayer. However, the hBN has a larger damage threshold power, but a weaker SHG intensity (Figure 5d). To determine the relationship between SHG and the packing direction of the crystal of **1** in Figure 5b, polarization-dependent SHG measurements were conducted. These experiments revealed a great contrast in the parallel component of SHG intensity along the packing direction of **1** (Figure 5e). In the wavelength-dependent two-photon excitation experiments with the excitation wavelength tuned from 760 to 930 nm, the SHG intensity of **1** exhibits a peak at ~800 nm (Figure 5f), which is correlated to its absorption spectrum (Figure S8).

In conclusion, a graphenic molecular bowl was concisely synthesized, and sextuple Se annulation at the bay positions

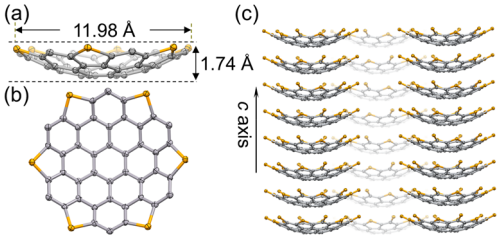

Figure 4. Crystal structure of **1**. (a, b) Side and top view of **1** without peripheral phenylseleno groups. (c) Side view of the crystal packing of **1**. The thermal ellipsoids are set at a probability level of 50%. The peripheral phenyl rings are omitted for clarity.

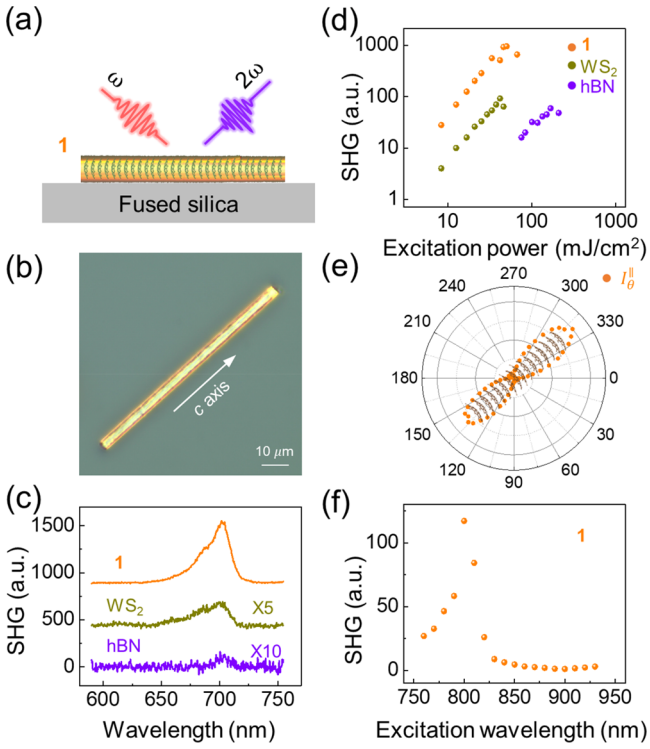

Figure 5. SHG performance of **1**. (a) Side-view illustration of crystal of **1** and its optical SHG. (b) Optical image of crystal **1**. (c) SHG spectra of **1**, WS_2 monolayer, and hBN monolayer under 1380 nm pulsed-laser excitation, respectively. (d) Measured SHG intensity of **1**, WS_2 monolayer, and hBN monolayer as a function of the excitation power under 1380 nm excitation, respectively. (e) Polarization-dependent SHG patterns measured on the crystal of **1**. (f) Wavelength-dependent SHG intensity of **1**. The wavelength-dependent SHG measurements were calibrated with the z-cut fused silica sample.

https://doi.org/10.1021/jacs.2c12401
J. Am. Chem. Soc. XXXX, XXX, XXX−XXX

was achieved by a one-pot reaction. The synthesis of **1** demonstrates the strategy of constructing graphenic bowls by pentagonal cyclization of the bay positions of armchair-edged aromatic hydrocarbons. The structural investigations of **1** revealed a unique bilayer stacked assembly of **1** in solution and gas phase, compared to other buckybowls, due to the enhanced interlayer interactions. **1** in the crystalline state forms synclastic one-dimensional columns, breaking the centrosymmetric symmetry, which consequentially gives its crystals significant SHG responses with a high polarization dependence. As a whole, synthesis of **1** could inspire the investigations of other graphenic nanocarbon bowls and provide a brand-new bowl-shaped building block for host−guest chemistry and non-centrosymmetric organic materials.

■ ASSOCIATED CONTENT

Supporting Information

The Supporting Information is available free of charge at https://pubs.acs.org/doi/10.1021/jacs.2c12401.

Experimental section, optical spectra, cyclic voltammogram, computation details, ^{1}H and ^{13}C NMR spectra. (PDF)

Accession Codes

CCDC 2214978 contains the supplementary crystallographic data for this paper. These data can be obtained free of charge via www.ccdc.cam.ac.uk/data_request/cif, or by emailing data_request@ccdc.cam.ac.uk, or by contacting The Cambridge Crystallographic Data Centre, 12 Union Road, Cambridge CB2 1EZ, UK; fax: +44 1223 336033.

■ AUTHOR INFORMATION

Corresponding Authors

Yuan-Zhi Tan − *State Key Laboratory of Physical Chemistry of Solid Surfaces, College of Chemistry and Chemical Engineering, Xiamen University, Xiamen 361005, China;* orcid.org/0000-0002-1268-2761; Email: yuanzhi_tan@xmu.edu.cn

Kaihui Liu − *State Key Laboratory for Mesoscopic Physics, Frontiers Science Centre for Nano-optoelectronics, School of Physics, Peking University, Beijing 100871, China;* orcid.org/0000-0002-8781-2495; Email: khliu@pku.edu.cn

Authors

Zhen-Lin Qiu − *State Key Laboratory of Physical Chemistry of Solid Surfaces, College of Chemistry and Chemical Engineering, Xiamen University, Xiamen 361005, China;* orcid.org/0000-0002-7590-5547

Yang Cheng − *State Key Laboratory for Mesoscopic Physics, Frontiers Science Centre for Nano-optoelectronics, School of Physics, Peking University, Beijing 100871, China*

Qi Zeng − *State Key Laboratory of Physical Chemistry of Solid Surfaces, College of Chemistry and Chemical Engineering, Xiamen University, Xiamen 361005, China*

Qiong Wu − *State Key Laboratory of Physical Chemistry of Solid Surfaces, College of Chemistry and Chemical Engineering, Xiamen University, Xiamen 361005, China*

Xin-Jing Zhao − *State Key Laboratory of Physical Chemistry of Solid Surfaces, College of Chemistry and Chemical Engineering, Xiamen University, Xiamen 361005, China*

Rong-Jie Xie − *State Key Laboratory of Physical Chemistry of Solid Surfaces, College of Chemistry and Chemical Engineering, Xiamen University, Xiamen 361005, China*

LiuBin Feng − *State Key Laboratory of Physical Chemistry of Solid Surfaces, College of Chemistry and Chemical Engineering, Xiamen University, Xiamen 361005, China*

Complete contact information is available at: https://pubs.acs.org/10.1021/jacs.2c12401

Author Contributions

#Z.-L.Q. and Y.C. contributed equally.

Notes

The authors declare no competing financial interest.

■ ACKNOWLEDGMENTS

This work was supported by the National Natural Science Foundation of China (92061103, 21721001, 51991342, 52025023, 22101241) and the China Postdoctoral Science Foundation (2020M682084).

■ REFERENCES

(1) Kroto, H. W.; Heath, J. R.; O'Brien, S. C.; Curl, R. F.; Smalley, R. E. C_{60}: Buckminsterfullerene. *Nature* **1985**, *318*, 162−163.

(2) Ugarte, D. Curling and Closure of Graphitic Networks under Electron-Beam Irradiation. *Nature* **1992**, *359*, 707−709.

(3) Iijima, S. Helical Microtubules of Graphitic Carbon. *Nature* **1991**, *354*, 56−58.

(4) Higashibayashi, S.; Sakurai, H. Asymmetric Synthesis of a Chiral Buckybowl, Trimethylsumanene. *J. Am. Chem. Soc.* **2008**, *130*, 8592−8593.

(5) Bandera, D.; Baldridge, K. K.; Linden, A.; Dorta, R.; Siegel, J. S. Stereoselective Coordination of C_5-Symmetric Corannulene Derivatives with an Enantiomerically Pure [Rh(I)(Nbd*)] Metal Complex. *Angew. Chem., Int. Ed.* **2011**, *50*, 865−867.

(6) Tan, Q.; Higashibayashi, S.; Karanjit, S.; Sakurai, H. Enantioselective Synthesis of a Chiral Nitrogen-Doped Buckybowl. *Nat. Commun.* **2012**, *3*, 891.

(7) Scott, L. T.; Hashemi, M. M.; Bratcher, M. S. Corannulene Bowl-to-Bowl Inversion Is Rapid at Room-Temperature. *J. Am. Chem. Soc.* **1992**, *114*, 1920−1921.

(8) Juricek, M.; Strutt, N. L.; Barnes, J. C.; Butterfield, A. M.; Dale, E. J.; Baldridge, K. K.; Stoddart, F.; Siegel, J. S. Induced-Fit Catalysis of Corannulene Bowl-to-Bowl Inversion. *Nat. Chem.* **2014**, *6*, 222−228.

(9) Jaafar, R.; Pignedoli, C. A.; Bussi, G.; Ait-Mansour, K.; Groening, O.; Amaya, T.; Hirao, T.; Fasel, R.; Ruffieux, P. Bowl Inversion of Surface-Adsorbed Sumanene. *J. Am. Chem. Soc.* **2014**, *136*, 13666−13671.

(10) Liu, Y. M.; Huang, Y. Q.; Liu, S. H.; Chen, D. D.; Tang, C.; Qiu, Z. L.; Zhu, J.; Tan, Y. Z. Bowl Inversion in an Exo-Type Supramolecule in the Solid State. *Angew. Chem., Int. Ed.* **2019**, *58*, 13276−13279.

(11) Furukawa, S.; Wu, J. Y.; Koyama, M.; Hayashi, K.; Hoshino, N.; Takeda, T.; Suzuki, Y.; Kawamata, J.; Saito, M.; Akutagawa, T. Ferroelectric Columnar Assemblies from the Bowl-to-Bowl Inversion of Aromatic Cores. *Nat. Commun.* **2021**, *12*, 768.

(12) Li, M. H.; Chen, X.; Yakiyama, Y.; Wu, J. Y.; Akutagawa, T.; Sakurai, H. Tuning the Dielectric Response by Co-Crystallisation of Sumanene and Its Fluorinated Derivative. *Chem. Commun.* **2022**, *58*, 8950−8953.

(13) Li, M. H.; Wu, J. Y.; Sambe, K.; Yakiyama, Y.; Akutagawa, T.; Kajitani, T.; Fukushima, T.; Matsuda, K.; Sakurai, H. Dielectric Response of 1,1-Difluorosumanene Caused by an In-Plane Motion. *Mater. Chem. Front.* **2022**, *6*, 1752−1758.

(14) Xiao, W.; Passerone, D.; Ruffieux, P.; Ait-Mansour, K.; Groning, O.; Tosatti, E.; Siegel, J. S.; Fasel, R. C60/Corannulene

on Cu(110): A Surface-Supported Bistable Buckybowl-Buckyball Host-Guest System. *J. Am. Chem. Soc.* **2008**, *130*, 4767−4771.
(15) Liu, Y. M.; Xia, D.; Li, B. W.; Zhang, Q. Y.; Sakurai, T.; Tan, Y. Z.; Seki, S.; Xie, S. Y.; Zheng, L. S. Functional Sulfur-Doped Buckybowls and Their Concave-Convex Supramolecular Assembly with Fullerenes. *Angew. Chem., Int. Ed.* **2016**, *55*, 13047−13051.
(16) Lampart, S.; Roch, L. M.; Dutta, A. K.; Wang, Y.; Warshamanage, R.; Finke, A. D.; Linden, A.; Baldridge, K. K.; Siegel, J. S. Pentaindenocorannulene: Properties, Assemblies, and C_{60} Complex. *Angew. Chem., Int. Ed.* **2016**, *55*, 14648−14652.
(17) Shoji, Y.; Kajitani, T.; Ishiwari, F.; Ding, Q.; Sato, H.; Anetai, H.; Akutagawa, T.; Sakurai, H.; Fukushima, T. Hexathioalkyl Sumanenes: An Electron-Donating Buckybowl as a Building Block for Supramolecular Materials. *Chem. Sci.* **2017**, *8*, 8405−8410.
(18) Lu, X.; Gopalakrishna, T. Y.; Han, Y.; Ni, Y.; Zou, Y.; Wu, J. Bowl-Shaped Carbon Nanobelts Showing Size-Dependent Properties and Selective Encapsulation of C_{70}. *J. Am. Chem. Soc.* **2019**, *141*, 5934−5941.
(19) Xu, Y. Y.; Tian, H. R.; Li, S. H.; Chen, Z. C.; Yao, Y. R.; Wang, S. S.; Zhang, X.; Zhu, Z. Z.; Deng, S. L.; Zhang, Q. Y.; Yang, S. F.; Xie, S. Y.; Huang, R. B.; Zheng, L. S. Flexible Decapyrrylcorannulene Hosts. *Nat. Commun.* **2019**, *10*, 485.
(20) Wu, J. R.; Zhang, G. Periphery-Core Strategy to Access a Bowl-Shaped Molecule Bearing Multiple Heteroatoms. *Angew. Chem., Int. Ed.* **2022**, *61*, e202208061.
(21) Wang, Y. J.; Rickhaus, M.; Blacque, O.; Baldridge, K. K.; Juricek, M.; Siegel, J. S. Cooperative Weak Dispersive Interactions Actuate Catalysis in a Shape-Selective Abiological Racemase. *J. Am. Chem. Soc.* **2022**, *144*, 2679−2684.
(22) Wu, Y. T.; Siegel, J. S. Aromatic Molecular-Bowl Hydrocarbons: Synthetic Derivatives, Their Structures, and Physical Properties. *Chem. Rev.* **2006**, *106*, 4843−4867.
(23) Majewski, M. A.; Stepien, M. Bowls, Hoops, and Saddles: Synthetic Approaches to Curved Aromatic Molecules. *Angew. Chem., Int. Ed.* **2019**, *58*, 86−116.
(24) Barth, W. E.; Lawton, R. G. Dibenzo[ghi,mno]fluoranthene. *J. Am. Chem. Soc.* **1966**, *88*, 380−381.
(25) Hanson, J. C.; Nordman, C. E. The Crystal and Molecular Structure of Corannulene, $C_{20}H_{10}$. *Acta Crystallogr.* **1976**, *B32*, 1147−1153.
(26) Ito, S.; Tokimaru, Y.; Nozaki, K. Benzene-Fused Azacorannulene Bearing an Internal Nitrogen Atom. *Angew. Chem., Int. Ed.* **2015**, *54*, 7256−7260.
(27) Yokoi, H.; Hiraoka, Y.; Hiroto, S.; Sakamaki, D.; Seki, S.; Shinokubo, H. Nitrogen-Embedded Buckybowl and Its Assembly with C_{60}. *Nat. Commun.* **2015**, *6*, 8215.
(28) Geim, A. K.; Novoselov, K. S. The Rise of Graphene. *Nat. Mater.* **2007**, *6*, 183−191.
(29) Amaya, T.; Hirao, T. Chemistry of Sumanene. *Chem. Rec.* **2015**, *15*, 310−321.
(30) Zou, Y.; Zeng, W.; Gopalakrishna, T. Y.; Han, Y.; Jiang, Q.; Wu, J. Dicyclopenta[4,3,2,1-ghi:4′,3′,2′,1′-pqr]perylene: A Bowl-Shaped Fragment of Fullerene C_{70} with Global Antiaromaticity. *J. Am. Chem. Soc.* **2019**, *141*, 7266−7270.
(31) Sakurai, H. A Synthesis of Sumanene, a Fullerene Fragment. *Science* **2003**, *301*, 1878−1878.
(32) Sakurai, H.; Daiko, T.; Sakane, H.; Amaya, T.; Hirao, T. Structural Elucidation of Sumanene and Generation of Its Benzylic Anions. *J. Am. Chem. Soc.* **2005**, *127*, 11580−11581.
(33) Chen, L.; Hernandez, Y.; Feng, X. L.; Mullen, K. From Nanographene and Graphene Nanoribbons to Graphene Sheets: Chemical Synthesis. *Angew. Chem., Int. Ed.* **2012**, *51*, 7640−7654.
(34) Li, X. X.; Zhu, Y. T.; Shao, J. F.; Wang, B. L.; Zhang, S. X.; Shao, Y. L.; Jin, X. J.; Yao, X. J.; Fang, R.; Shao, X. F. Non-Pyrolytic, Large-Scale Synthesis of Trichalcogenasumanene: A Two-Step Approach. *Angew. Chem., Int. Ed.* **2014**, *53*, 535−538.
(35) Tan, Q. T.; Zhou, D. D.; Zhang, T.; Liu, B. X.; Xu, B. Iodine-Doped Sumanene and Its Application for the Synthesis of Chalcogenasumanenes and Silasumanenes. *Chem. Commun.* **2017**, *53*, 10279−10282.
(36) Jiang, M.; Guo, J.; Liu, B.; Tan, Q.; Xu, B. Synthesis of Tellurium-Containing π-Extended Aromatics with Room-Temperature Phosphorescence. *Org. Lett.* **2019**, *21*, 8328−8333.
(37) Wang, S. T.; Yan, C. X.; Shang, J. H.; Wang, W. B.; Yuan, C. S.; Zhang, H. L.; Shao, X. F. Doping Sumanene with Both Chalcogens and Phosphorus(V): One-Step Synthesis, Coordination, and Selective Response Toward Ag-I. *Angew. Chem., Int. Ed.* **2019**, *58*, 3819−3823.
(38) Tan, Y. Z.; Osella, S.; Liu, Y.; Yang, B.; Beljonne, D.; Feng, X. L.; Mullen, K. Sulfur-Annulated Hexa-peri-hexabenzocoronene Decorated with Phenylthio Groups at the Periphery. *Angew. Chem., Int. Ed.* **2015**, *54*, 2927−2931.
(39) Zhao, X.-J.; Hou, H.; Fan, X.-T.; Wang, Y.; Liu, Y.-M.; Tang, C.; Liu, S.-H.; Ding, P.-P.; Cheng, J.; Lin, D.-H.; Wang, C.; Yang, Y.; Tan, Y.-Z. Molecular bilayer graphene. *Nat. Commun.* **2019**, *10*, 3057.
(40) Rieger, R.; Mullen, K. Forever young: polycyclic aromatic hydrocarbons as model cases for structural and optical studies. *J. Phys. Org. Chem.* **2010**, *23*, 315−325.
(41) Stabel, A.; Herwig, P.; Müllen, K.; Rabe, J. P. Diodelike Current−Voltage Curves for a Single Molecule−Tunneling Spectroscopy with Submolecular Resolution of an Alkylated,peri-Condensed Hexabenzocoronene. *Angew. Chem., Int. Ed.* **1995**, *34*, 1609−1611.
(42) Herwig, P. T.; Enkelmann, V.; Schmelz, O.; Mullen, K. Synthesis and structural characterization of hexa-tert-buty-hexa-peri-hexabenzocoronene, its radical cation salt and its tricarbonylchromium complex. *Chem.—Eur. J.* **2000**, *6*, 1834−1839.
(43) Zhang, Q.; Prins, P.; Jones, S. C.; Barlow, S.; Kondo, T.; An, Z. S.; Siebbeles, L. D. A.; Marder, S. R. Fluorine-substituted hexakisdecyloxy-hexa-peri-hexabenzocoronene. *Org. Lett.* **2005**, *7*, 5019−5022.
(44) Priyakumar, U. D.; Sastry, G. N. First Ab Initio and Density Functional Study on the Structure, Bowl-to-Bowl Inversion Barrier, and Vibrational Spectra of the Elusive C-3*v*-Symmetric Buckybowl: Sumanene, $C_{21}H_{12}$. *J. Phys. Chem. A* **2001**, *105*, 4488−4494.
(45) Caracelli, I.; Zukerman-Schpector, J.; Tiekink, E. R. T. Supramolecular aggregation patterns based on the bio-inspired Se(lone pair)··· pi(aryl) synthon. *Coord. Chem. Rev.* **2012**, *256*, 412−438.
(46) Kong, X.; Zhou, P. P.; Wang, Y. Chalcogen···π Bonding Catalysis. *Angew. Chem., Int. Ed.* **2021**, *60*, 9395−9400.
(47) Li, Y.; Rao, Y.; Mak, K. F.; You, Y.; Wang, S.; Dean, C. R.; Heinz, T. F. Probing Symmetry Properties of Few-Layer MoS_2 and h-Bn by Optical Second-Harmonic Generation. *Nano Lett.* **2013**, *13*, 3329−3333.
(48) Yao, K.; Finney, N. R.; Zhang, J.; Moore, S. L.; Xian, L.; Tancogne-Dejean, N.; Liu, F.; Ardelean, J.; Xu, X.; Halbertal, D.; Watanabe, K.; Taniguchi, T.; Ochoa, H.; Asenjo-Garcia, A.; Zhu, X.; Basov, D. N.; Rubio, A.; Dean, C. R.; Hone, J.; Schuck, P. J. Enhanced Tunable Second Harmonic Generation from Twistable Interfaces and Vertical Superlattices in Boron Nitride Homostructures. *Sci. Adv.* **2021**, *7*, eabe8691.

https://doi.org/10.1021/jacs.2c12401
J. Am. Chem. Soc. XXXX, XXX, XXX−XXX